Cryptotanshinone Breaks ERα-dependent and -independent BCRP Dimerization to Reverse the Multidrug Resistance in Breast Cancer

Wenting Ni
Nanjing University of Chinese Medicine
Hui Fan
Nanjing University of Chinese Medicine
Xiuqin Zheng
Nanjing University of Chinese Medicine
Fangming Xu
Nanjing University of Chinese Medicine
Yuanyuan Wu
Nanjing University of Chinese Medicine
Xiaoman Li
Nanjing University of Chinese Medicine
Aiyun Wang
Nanjing University of Chinese Medicine
Shile Huang
Louisiana State University Health Sciences Center
Wenxing Chen (chenwx@njucm.edu.cn)
Nanjing University of Chinese Medicine https://orcid.org/0000-0003-4571-7622
Shijun Wang
Shandong University of Traditional Chinese Medicine
Yin Lu
Nanjing University of Chinese Medicine

Research

Keywords: Cryptotanshinone, Breast cancer resistance protein, Estrogen Receptor α, Multidrug resistance

Posted Date: September 24th, 2020

DOI: https://doi.org/10.21203/rs.3.rs-80705/v1

Abstract

Background

Not only a long-term anti-estrogen therapy, but also estrogen receptor-negative breast cancer are generally prone to induce resistance, causing poor prognosis in clinic. Breast cancer resistance protein (BCRP) plays an important role in multidrug resistance. Here it is to elucidate the mechanism that a natural compound cryptotanshinone inhibits BCRP.

Methods

HPLC was for analyzing the special compound concentration and molecular docking assay for the affinity of compound with protein. Non-reducing gradient gel electrophoresis and fluorescence resonance energy transfer (FRET) microscopy imaging were used to detect polymer and stain the membrane protein. Immunofluorescence staining, plasmids transfection, real-time PCR and western blot were also used.

Results

Cryptotanshinone, an anti-estrogen compound was firstly found to inhibit breast cancer resistance protein (BCRP) membrane dimerization to attenuate its transport function. And this process is dependent on estrogen receptor α (ERα) in breast cancer. Furthermore, the resistant breast cancer cells with high BCRP expression are also sensitive to cryptotanshinone because it can bind to BCRP and significantly inhibit membrane dimer of BCRP although they are ERα-negative, suggesting that BCRP expression is essential to cryptotanshinone reversing the resistance; Meanwhile, the combination of cryptotanshinone and chemotherapy drugs could obviously enhance the chemotherapeutic effect.

Conclusion

Cryptotanshinone is a novel natural BCRP inhibitor via blocking the formation of BCRP membrane dimer by an ERα-dependent and -independent way. Cryptotanshinone reverses resistance dependent on BCRP in breast cancer.

1. Background

Chemotherapy is one of the foremost methods to treat cancer nowadays, but the occurrence of multidrug resistance (MDR) has made its current clinical application become increasingly limited[1]. The MDR of breast cancer is prominent in all tumor resistance, especially in estrogen receptor α-positive (ERα+) breast cancer patients. After receiving endocrine therapy such as tamoxifen, about 70% patients will have recurrence of drug resistance in the late stages[2]. In recent years, many studies have shown that there is a

close relationship between the occurrence of breast cancer MDR and the ATP-binding cassette (ABC) transporter family, especially P-glycoprotein (P-gp/ABCB1), multidrug-resistance-associated protein 1 (MRP1/ABCC1) and the breast cancer resistance proteins (BCRP/ABCG2) play key roles in the development of breast cancer MDR[3, 4].

ABCG2, the subfamily G of the human adenosine triphosphate (ATP)-binding cassette (ABC) transporter superfamily, was known as BCRP[5]. Its structure is similar to P-gp and MRP1, certain homologous sequences and the role of "drug pump" in function[6]. However, BCRP still has its own unique conformation, a nucleotide binding domain (Nucleotide-binding domain (NBD) at the C-terminus and a hydrophobic transmembrane domain (TMD) at the N-terminus, which determined BCRP as a semi-transporter[7]. In general, P-gp and MRP1 that have two NBDs and TMDs structures called full transporters[8]. Semi-transporters are commonly localized in cytoplasm, but BCRP was the first reported semi-transporter localized on the cell membrane[9]. Several studies indicated that BCRP was likely to form homodimers, tetramers, dodecamers, and even larger oligomer structures by intramolecular disulfide linkages. It significantly increases the efficiency of external pumping by increasing the formation of the outer channel cavity[10]. Thus, inhibition of BCRP and blocking the efflux of therapeutic drugs has been considered a feasible strategy for eliminating the MDR, this boosts the development of BCRP inhibitors[11].

Cryptotanshinone (CPT) is a natural diterpenoid from the *Salvia miltiorrhiza.* Since CPT was firstly demonstrated to exhibit anti-cancer activity dependent on inhibition of STAT3 dimer[12], its molecular mechanism attracted much concern. We also made much attempt on it, and found that CPT can not only inhibit mTOR signaling[13], but also activate MAPK pathways[14], leading to cell death. However, CPT is not an mTOR inhibitor like rapamycin and its derivatives, but inhibits mTOR signaling via activating AMPK-TSC2 axis[15]. Recently, we found that CPT indicates a significant inhibition on MCF-7 but not MDA-MB-231 cells by an ERα-dependent way. Furthermore, MCF-7/ADR, a doxorubicin-induced multidrug-resistant cell line, is also sensitive to CPT, and CPT can distinctly enhance the inhibitory effect of tamoxifen on MCF-7/ADR[16]. As we knew, MCF-7/ADR cells with high expression of ABC protein family but negative ERα expression are induced by doxorubicin to acquire multidrug resistance. Therefore, we judged that the ERα and BCRP are the essential factors mediating CPT reversing MDR.

In this study, we for the first time found the natural compound CPT can inhibit the dimerization of BCRP in the membrane by an ERα-dependent way in ERα-positive breast cancer cells. However, it can directly block BCRP dimerization in ERα-negative resistant breast cancer cells to reverse the resistance. It can be a potential agent for application in both ERα-positive and ERα-negative breast cancer with high expression and decreasing the possibility of resistance.

2. Materials And Methods

2.1 Chemicals and reagents

CPT (purity 98%, HPLC, Xian Yuxuan Biotechnology Co., Ltd.), RPMI 1640, Dulbecco's Modified Eagle Medium (DMEM), fetal bovine serum (FBS), Opti MEM medium, trypsin-EDTA and penicillin/streptomycin were purchased from Gibco (Grand Island, NY, USA). KO143, was obtained from MCE (Newark, NJ, USA). Non-denaturing non-reducing protein Beyotime Biotechnology (Shanghai, China). Mitoxantrone was brought from Meilunbio (Dalian, Liaoning, China). Rhodamine123 was purchased from Sigma-Aldrich (St. Louis, MO, USA). Doxorubicin was obtained from Bairui Biotechnology (Nanjing, China). Goat Anti-Rabbit IgG H&L FITC (Abcam, Cambridge, UK). MTS, BSA were provided by Biosharp (Hefei, Anhui, China). RIPA, PMSF were given by Dingguo Biotechnology (Beijing, China).

2.2 Cell culture

Human breast cancer cells (MCF-7 cells and MDA-MB-231 cells) were obtained from American Type Culture Collection (Manassas, VA, USA). MCF-7 cells were cultured in 1640 with 10% FBS and MDA-MB-231 cells were cultured in DMEM with 10% FBS. Doxorubicin multidrug resistant cell line MCF-7/ADR cells were purchased from Nanjing BERKE Biology Co., Ltd. MCF-7/ADR cells were cultured in 1640 with 10% FBS and 1.25 μg/ml doxorubicin. All of them were grown in a 5% CO_2 and 95% air humidified atmosphere.

2.3 Cell viability assay

MCF-7 cells, MDA-MB-231 cells, MCF-7/ADR cells were seeded in a 96-well plate at a density of 1×10^4/well. After treating with drug or reagent, MTS (1:10 dilution in serum-free medium) was added and incubated at 37 °C for 4 h. Finally, the formazan was dissolved in DMSO and cell viability was evaluated through measuring the optical density (OD) at 490 nm using the BioTek Synergy2 microplate reader (BioTek Instruments, VT, USA).

2.4 HPLC analysis

CPT concentration was measured using HPLC. Cell lysates were extracted in the extraction buffer (containing methanol: water (1:1, v/v)) in the cold room for 15 min, followed by scraping and centrifuging at 17000 g for 10 min. CPT analysis was performed by HPLC (Waters E2695, Separations Module). Samples were injected into a 4.6mm × 250 mm Stable Bond column (ZORBAX Eclipse Plus C18; Agilent, CA, USA). The chromatography was run started with 45% solution A (methanol) and 55% solution B (H_2O), and the volume (%) of solution A was raised to 50, 90, 100 at 10 min, 30 min, and 35 min respectively. Finally, the situation comes back to 45% solution A when the time of 45 min, and then holding up until stopped. Data were collected and analyzed by Analyst Software (AB Sciex).

2.5 Molecular docking assay

The three-dimensional structure of cryptotanshinone and mitoxantrone was achieved from PubChem Compound database (https://www.ncbi.nlm.nih.gov/pccompound/). Meanwhile, the structure of BCRP/ABCG2 (Protein Data Bank (PDB) ID: 6FFC with resolution of 3.56 Å) was retrieved from the Research Collaborator for Structural Bioinformatics PDB (Anonymous, www.rcsb.org). The molecular docking between the two compounds and BCRP/ABCG2 were evaluated by Discovery Studio (DS) 3.5

using the CDOCKER Protocol under the protein–ligand interaction section after preparing protein and ligands. The poses were scored by CDOCKER interaction energy, and the binding sites were also be showed.

2.6 Plasmids and transient transfection

The ERα shRNA (sense: 5'-GATCCCGCTACTGTTTGCTCCTAACCTCGAGGTTAGGAGCAAACAGTAGCTTTTTGGAT-3'; Antisense: 3"AGCTATCCAAAAAGCTACTGTTTGCTCCTAACCTCGAGGTTAGGAGCAAACAGTAGCGG-5')[16] was synthesized by Genechem (Shanghai, China). MCF-7 cells were planted in 6-well plates at a density of 3×10^5cells/well. The ERα shRNA plasmid (888 ng/μL) were diluted in Opti-MEM (100μL) and then mixed with lipofectamine 2000 reagent (Life Technologies, NY, USA). After 6 h transfection, culture medium was changed to normal medium and sequentially incubated in 37 °C for 16 h. The Con-shRNA (535 ng/μL) was used as a negative control.

2.7 MX/Rh123/DOX/TOPO efflux experiment

The mitoxantrone (MX)/rhodamine/doxorubicin (DOX)/Topotecan (TOPO) efflux experiment were performed following the modified method as reference described[17]. Briefly, breast cancer cells (3×10^5 cells per well) were seeded in 6-well plates and incubated overnight. When the cell confluence reached about 80%, the drug was added. After the administration, the cells were collected by centrifugation in 2 ml tubes, and each tube was added with 1 ml of serum-free medium to homogenize the cells. Then, all the cells except the blank group were added with the corresponding compounds and incubated in the dark under 37 °C for 30 min. (The MX positive group given KO143 10 μmol/L for 15 min in advance). After the end of time, all cells were undergone 1500 rpm, 4 °C, 5 min centrifugation, and the supernatant was discarded. Then washed cells with pre-cooled PBS twice. Finally, resuspending cells with 400μL pre-cooled PBS to test. The fluorescence accumulation of MX/Rh123/DOX/TOPO is detected by BD Accuri C6 Flow Cytometry (Becton, Dickinson and Company, NY, USA). The detection channel was FL-4/FL-1/FL-2.

2.8 Non-reducing gradient gel electrophoresis

The non-reducing gradient gel electrophoresis was performed following the modified method as reference described[18]. After the end of the cell administration, membrane protein and cytoplasmic protein are extracted as described in 2.11. The protein samples were denatured with loading buffer that containing no reducing agents such as DTT or 2-ME. Samples were boiled at 100 °C for 15 min. And the remaining steps were essentially identical to western blotting. When detecting the BCRP polymer, membrane proteins were separated by 6% Tris-glycine SDS-PAGE and molecular weight markers were used multicolor broad range protein ladder ranging from 10 kDa to 260 kDa (Thermo Scientific, Waltham, MA, USA).

2.9 Fluorescence resonance energy transfer (FRET) microscopy imaging

The FRET method referred to several references and performed after appropriate modification[19]. The pCFP-ABCG2 plasmid and pYFP-ABCG2 plasmid were a gift from M.S. Jun Wang, Drug Discovery and Design Center, Shanghai Institute of Materia Medica, Chinese Academy of Sciences (Shanghai, China). The breast cancer cells were seeded in a 35 mm diameter confocal culture dish, and when the cell confluence reached to 70%, the plasmid transfection was performed. The cell transfection steps were primarily based on the protocol provided by manufacturer (Invitrogen, NY, USA). Plasmid pCFP-ABCG2 (191.3 ng/μL), pYFP-ABCG2 (399.3 ng/μL) and 3μL lipofectamine 2000 reagent (Life Technologies, NY, USA) were respectively mixed with 50μL Opti-MEM medium. After incubating for 5 min at room temperature, the above two mixtures were lightly mixed and cultured for 10 min at room temperature. Finally, the 100μL mixture was added dropwise to 1 ml serum-free medium, and 100μL FBS was added 6 hours later, then incubation was continued for 16 hours at 37 °C. After successfully transfection, the drug could be administrated. Finally, the living cell FRET image were collected by Leica inverted fluorescence microscope (Leica Microsystems, Solms, Germany) and analyzed by Image J software.

2.10 Immunofluorescence staining

Cells were plated on glass coverslips in 6-well plates and then treated with corresponding drug or reagents. First, stain the cell membrane with 10 μmol/L DiI (Beyotime Biotechnology, Shanghai, China) for 10 min at 37 °C. After that, cells were fixed in 4% paraformaldehyde for 20 min, blocked in BSA (1% BSA dissolved in PBS). Cells were incubated with corresponding primary antibody (1:100 dilution) overnight at 4 °C, followed by incubation with Goat Anti-Rabbit IgG H&L FITC (1:1000 dilution) for 2 h and Hoechst nuclear dye for 10 min in dark. The images were obtained from laser scanning confocal microscope (Leica TCS SP5 X, Solms, Germany).

2.11 Cell membrane protein and cytoplasmic protein extraction

Cell membrane protein and cytoplasmic protein were extracted according to the protocol provided by manufacturer (Beyotime Biotechnology, Shanghai, China). In brief, cells were seeded into a culture dish (Lab services, Waltham, MA, USA) with diameter of 150 mm, and treated with compounds when the cell coverage area reached about 80%. After the time of the administration, it was washed once with ice PBS, and then the cells were scraped off with scraper, collected in a centrifuge tube, 4 °C, 600 g, 5 min. Discarding supernatant and resuspending cell pellet with reagent A added with PMSF (1:100 dilution), and placed in ice bath about 10–15 min. Then, the cells were disrupted by liquid nitrogen, freezing and thawing twice, and centrifuged at 4 °C, 700 g, 10 min. The supernatant was collected, 4 °C, 14,000 g, 30 min to precipitate cell membrane fragments. The supernatant was cytoplasmic protein. The bottom cell pellet was resuspended with reagent B, vortexed 5 s, ice bath 5–10 min. Finally, 4 °C, 14,000 g, 5 min, the supernatant was cell membrane protein, which was stored at -80℃. Cells were centrifuged by Beckman Microfuge® 20R (Beckman Coulter, MA, USA).

2.12 Western blotting analysis

Western blot was performed and analyzed according to the reference[15]. The primary antibodies were used as follows: ERα, BCRP/ABCG2, MDR1/ABCB1 (Cell Signaling Technology, Danvers, MA, USA), GAPDH (Bioworld Technology, MN, USA). ABCC1 (Affinity, MA, USA) HRP-Goat Anti-rabbit IgG(H + L) was purchased from Bioworld Technology Company.

2.13 RNA isolation and real-time PCR

The RNA isolation experiment was mainly carried out according to manufacturer's guidelines. Total RNA was extracted from MCF-7 cells or MDA-MB-231 cells with Trizol (Vazyme, Nanjing, China) and then reversely transcribed to cDNA by HiScript® II Reverse Transcriptase (Vazyme, Nanjing, China). Real-Time PCR was executed of the ChamQTM SYBR® qPCR Master Mix (Vazyme, Nanjing, China), using Applied Biosystems 7500 Real-Time PCR Systems (Thermo Scientific, Waltham, MA, USA). GAPDH was considered as an invariant control, and mRNA levels were expressed as fold changes after normalizing to GAPDH. Table 1 listed out the primers (Sangon Biotech, Shanghai, China) used.

2.14 Statistical analysis

The results were determined using Student's t test (two-group comparison) and ANOVA test by GraphPad Prism 5.0 software. $P < 0.05$ was considered to be statistically significant.

3. Results

3.1 Intracellular accumulation of CPT is possibly related to BCRP

In order to further investigate the reasons why MCF-7 and MDA-MB-231 cells show different sensitivity to CPT except dependence on the ERα, we first detected the intracellular and extracellular CPT levels in both cell lines by HPLC. As indicated in (Fig. 1A), following the increase of CPT concentration, the intracellular and extracellular CPT level have a sharp increase and almost equal in MCF-7 cells, while in MDA-MB-231 cells the intracellular CPT level just indicates a slight fluctuation at a low level and is greatly lower than the extracellular level. And the difference is significant when the CPT concentration is up to more than 10 μmol/L (Fig. 1B). This result suggested that there is a certain transporter which regulates the intake and pumping process of CPT in cells. The most studied transporter proteins are ATP-binding transporters nowadays, and the main family members are P-gp, MRP1, BCRP and so on. We analyzed the expression of these three transporters in many cell lines from multi human tissues with the Human Protein Altas Database. The analysis indicated that BCRP/ABCG2 was highly expressed in MCF-7 cells (Fig. 1C), whereas P-gp/ABCB1 was almost not expressed and MRP1/ABCC1 was lowly expressed (Fig. 1D, E). Upon the abovementioned results, we speculated that BCRP may play an important regulatory role in transporting CPT across the membrane.

3.2 CPT inhibits efflux function of BCRP dependent on ERα

The close relationship between CPT and BCRP encouraged us to further explore the specific regulation of CPT on BCRP. Firstly, CPT has no significant effect on the total protein expression of BCRP in both cells (Fig. 2A, B). In addition, no significant effect was found on ABCG2 mRNA levels in MCF-7 and MDA-MB-231 cells by q-PCR (Fig. 2C, D; Table S1). These results prompted us to continue thinking whether CPT possibly influences the function of BCRP. Considering the most important ability of BCRP is to transport substrate, so it is necessary to examine this function. We evaluated the efflux function of BCRP through the mitoxantrone efflux experiment [20]. The results showed that the fluorescence peak of CPT-administered group in MCF-7 cells was significantly shifted to right compared with the control group (Fig. 2E, F). The fluorescence abundance of intracellular mitoxantrone increased represents the efflux function of BCRP was inhibited. However, the same phenomenon was not observed in MDA-MB-231 cells (Fig. 2G, H). So we suspected that the difference between the two cells would be related to the expression of ERα? Thus, we silenced the ERα expression in MCF-7 cells and then co-incubated with CPT for 8 hours (Fig. 2I). We found that the original efflux inhibition effect was partially reversed (Fig. 2J, K). These results verified that CPT does not affect the total protein and transcription level of BCRP/ABCG2, but can specifically inhibit the efflux function of BCRP in MCF-7 cells, and this effect is closely relevant with the presence of ERα.

3.3 CPT reduces membrane expression of BCRP

Particularly, BCRP is the first semi-transporter found to be localized on the cell membrane to function by an oligomer[21]. So it is necessary to know whether CPT affects the membrane BCRP and its oligomer. We extracted the membrane proteins and cytoplasmic proteins from MCF-7 and MDA-MB-231 cells for western blot analysis. The results showed that CPT can significantly inhibit the membrane protein expression of BCRP, but not the cytoplasm expression in MCF-7 cells (Fig. 3A, B). And the BCRP expression in cell membrane or in cytoplasm in MDA-MB-231 cells was not affected (Fig. 3C, D). It undoubtedly further illustrates the effect of CPT on BCRP function. In addition, we also used LCSM to co-localize BCRP protein with cell membrane. The findings were consistent with western blot results, indicating that CPT can significantly inhibit the enrichment of BCRP on MCF-7 cell membrane. As seen in Fig. 3E, when high concentrations of CPT were used (10 μmol/L, 20 μmol/L), The enrichment of FITC-BCRP on the cell membrane dyed with DiI were obviously inhibited. But this phenomenon was also not observed in MDA-MB-231 cells (Fig. 3F). Additionally, we confirmed the role of ERα during this process again. When ERα was silenced in MCF-7 cells, the enrichment of BCRP on the cell membrane increased, and there was still no significant change in cytoplasm (Fig. 3G, H). In hence, CPT inhibits the efflux function of BCRP through decreasing its expression in MCF-7 cell membrane, and ERα is essential.

3.4 CPT inhibits BCRP oligomer formation

We continued to evaluate the CPT effect on BCRP oligomer using the assay of non-reducing gradient gel electrophoresis. As shown in the Fig. 4A, BCRP on the membrane of MCF-7 was mainly in the form of dimers and oligomers (molecular weight over 140 kDa). Oligomer formation was significantly inhibited

when treated with CPT (10, 20 μmol/L). The Fig. 4B shows that although BCRP exists in the cytoplasm of MCF-7 cells, its main form is a non-functional monomer with a molecular weight of 70 kDa. Besides, we also applied FRET assay to further ensure the effect of CPT on the BCRP oligomer formation on cell membrane surface. We transfected the gene sequence ABCG2 labeled with CFP and YFP into MCF-7 or MDA-MB-231 cells. After confirming the pCFP-ABCG2 and pYFP-ABCG2 successfully translated and distributed in the cell membrane (Fig. 4C), CPT was given for 8 h and then photographed. If BCRP can form oligomers, FRET phenomenon will occur (Fig. 4D), and we can judge the formation of BCRP oligomers by FRET efficiency. Finally, the experimental results are consistent with non-reducing electrophoresis. CPT can destroy BCRP oligomer formation in MCF-7 cells (Fig. 4E, F), but has no significant effect in MDA-MB-231 cells (Fig. 4G, H). CPT can inhibit the membrane BCRP oligomer formation, ultimately stop functional efflux.

3.5 CPT inhibits BCRP in resistant breast cancer cells independent on ERα

Previously, it was found that doxorubicin-resistant breast cancer cells MCF-7/ADR are sensitive to CPT. As indicated in Fig. 5A, BCRP expresses highly in MCF-7/ADR, but lowly in MDA-MB-231 cells with a significance upon the interactive comparation. Combined with current researches, we try to explore whether CPT inhibits MCF-7/ADR cells also dependent on BCRP. Firstly, HPLC analysis found that the concentration of intracellular CPT nearly equals to the extracellular CPT in MCF-7/ADR cells (Fig. 5B). This result made us convinced that the transporters were involved in the inhibition of MCF-7/ADR cell proliferation by CPT. Due to the high expression of P-gp and MRP1 in MCF-7/ADR cells, we also found that CPT does not inhibit P-gp, MRP1 membrane protein and cytoplasmic protein expression by western blot (Fig.S1A, B, C, D) and also not affect the P-gp, MRP1 efflux function by the flow cytometry (Fig.S1E, F, G). So, excluding P-gp and MRP1 proteins, we paid attention to BCRP. Verified by a series of experiments, we knew that CPT also has no significant effect on the total protein expression of BCRP in MCF-7/ADR cells (Fig. 5C), but strongly inhibits the membrane protein expression of BCRP even at low concentration of 5 μmol/L (Fig. 5D). The cytoplasm has less BCRP content, but it could be observed that CPT can increase the BCRP content in the cytoplasm to some extent (Fig. 5E). Similarly, flow cytometry results showed that CPT could inhibit the efflux function of BCRP in MCF-7/ADR cells, especially at the high concentration of 20 μmol/L (Fig. 5F, G). FRET experiments also demonstrated that CPT inhibits the formation of BCRP oligomers in MCF-7/ADR cells too (Fig. 5H, I). It is worth noting that functional inhibition of BCRP by CPT requires ERα mediation in MCF-7 cells, whereas MCF-7/ADR cells have undergone many changes in morphology, characteristics and functions compared with parental MCF-7 cells. Above all, the most obvious change is the absence of ERα expression in MCF-7/ADR cells. This information suggested CPT may have a diverse approach to functional inhibition of BCRP. ERα expression or deletion is not the only criterion for judgment.

BCRP consists of a nucleotide binding domains (NBDs) and a transmembrane domains (TMDs)[7], TM1-3 are substrate binding regions (Fig. 5J). To further determine whether CPT can be recognized by BCRP and

extracellularly pumped out, we used molecular docking technology to dock mitoxantrone, the specific substrate of BCRP, with the protein 3D structure (Fig.S2A, B). After confirming the drug binding pocket, the CPT 3D structure was embedded for docking (Fig. 5K, L). As shown in Fig. 5K & Fig.S2A, through the intermolecular force comparison and calculation, the common binding sites were found to be VAL401, PHE439, LEU405, PHE432, PHE439. These results indicated CPT can be recognized by BCRP and extracellularly pumped out. The whole transport simulation process is shown in the Fig. 5M. When the substrate is bound into the cavity 1, the conformation of the protein changes with the transition from inward open to outward open. NDB combines with ATP hydrolysis to provide energy for conformational changes in the protein, while the substrate is transferred into the cavity 2, which has a relatively weak binding force, and the drug finally be pumped out. Taken together, CPT can bind to BCRP but plays an antagonized role for external pumping and the process is blocked leading to an accumulation of CPT in MCF-7 cells.

3.6 CPT enhances cancer cells sensitivity combined with BCRP efflux anti-cancer drugs

Based upon the above results, we immediately thought whether the synergistic effect would generate from the combination of CPT and anti-cancer drugs of BCRP efflux. To verify this assumption, we selected two of the most classic BCRP efflux drugs, mitoxantrone and topotecan[22]. At first, we screened the concentration of CPT and the positive control drug Ko143. Then, we carried out a 72-h co-incubation experiment at a concentration of 1 μmol/L which had no significant effect on the proliferation of MCF-7/ADR cells (Fig. 6A, B). Compared with the single-incubation group of mitoxantrone (Fig. 6C), topotecan (Fig. 6D), the co-incubation group with CPT could significantly reverse drug resistance at higher doses (mitoxantrone-10 μmol/L, topotecan-0.5 μmol/L and 1 μmol/L), and the inhibition rate of proliferation was under 50% which is close to Ko143 (Fig. 6E-6F). Meanwhile, subsequent flow cytometry showed that when mitoxantrone co-incubated with CPT, the accumulation of mitoxantrone in MCF-7/ADR cells was increased, that is, the functional inhibition of BCRP by CPT made the drugs efflux reduced (Fig. 6G, H). And the similar significant results were repeated with co-incubation of CPT and topotecan (Fig. 6I, J). In conclusion, CPT could enhance the sensitivity of the cells to anti-cancer drugs leading to reverse multi-drug resistance.

4. Discussion

The role of estrogen receptor-α (ERα) in breast cancer is well understood. ER expression is a critical factor for hormonal therapy and also considered as a prognostic marker. Nowadays, about 75% of breast cancer patients are ER-positive and administrated with anti-estrogen drugs, such as the selective estrogen receptor modulators tamoxifen. However, a part of ERα-positive breast cancers become hormone resistant with ERα-negative expression, and a majority of these patients suffered relapse in five years[23]. Furthermore, many researchers also found some chemotherapeutic agents may be less effective in $ERα^+$ breast cancer patients than $ERα^-$ ones[24]. These bidirectional results caused the complexity of the role of ERα in the resistant breast cancer.

Generally, the breast cancer resistance would be developed to multi-drug resistance, also called cross resistance. Several factors including ATP-binding cassette (ABC) transporters[5], the mutation of targeted oncogenes, survived cancer stem cells (CSCs)[25], activated cell growth factors are possibly involved in MDR. Specially, BCRP, one type of the ABC transporters is an important factor controlling the breast cancer MDR. Indeed, the relationship between ERα and BCRP expression has been investigated[26]. The estrogen response element (ERE) and progesterone response element (PRE) exist in the promoter region of BCRP[27]. The excessive transcriptional expression of this type of response element may play a major role in the development of breast cancer MDR[11]. The MDR is a multi-factor, multi-way, multi-stage and comprehensive process[28]. This study focused on BCRP primarily, and expected to look for new applications of CPT to reverse breast cancer MDR.

In the previous research, we have proved that CPT is not a selective estrogen receptor inhibitor though it can bind ERα and produce tamoxifen-like effect on cancers[16]. More importantly, CPT inhibits resistant MCF-7/ADR cells although it can activate MAPK and AKT, suggesting that induction of resistance via activation of MAPK[29] and AKT[30] is unavailable for CPT and there must be other factors involved in. So we judged BCRP is the key molecule mediating CPT reverse of the resistance. At present, a lot of BCRP inhibitors including highly selective inhibitors and non-selective inhibitors have been identified, and some highly selective inhibitors should be prospectively applied in clinic for reversing the MDR[31]. However, it is not completely clear to understand the molecular mechanism of BCRP inhibition. Certainly,it is known that some inhibit BCRP through inhibiting its ATPase activity, such as FTC, Ko134 and Ko143, while others as BCRP substrates can bind to BCRP and play a competitive role in suppressing transport function of BCRP[9, 31].

CPT indicates a different inhibition on BCRP. Primarily, breaking the BCRP dimerization in the membrane and inactivating its function contributes to its efflux blocked. Secondly, in $ERα^+$ MCF-7 cells, inhibition of BCRP oligomer is mediated by ERα, downregulation of ERα can decrease the accumulation of MX in cells, indicating the function of BCRP is enhanced. In $ERα^-$ MCF-7/ADR cells, BCRP membrane expression and oligomer were both inhibited. However, in MDA-MB-231 cells with negative ERα and low BCRP expression, CPT doesn't affect its proliferation. These data make a conclusion that CPT reversing resistance of breast cancer is dependent on BCRP, the higher expression of BCRP, the stronger inhibition effect on breast cancer cells. Although CPT is an anti-estrogen compound, ERα becomes an unnecessary mediator because CPT can directly bind BCRP to block efflux. Additionally, it was found that breast cancer cells can switch between ERα and ErbB signaling to induce resistance, combined inhibition of both signal can postpone resistance[32]. From MCF-7 to MCF-7/ADR, ERα is nearly silenced but BCRP significantly overexpressed. These suggest that there are two modes of CPT inhibition BCRP: ERα-dependent and ERα-independent. CPT switches the targets between ERα and BCRP to attenuate resistance.

Nowadays, more and more researchers thought that drugs invented or designed for individual molecular target cannot generally conquer multigenic diseases such as cancer, diabetes, hypertension, neural diseases and so on[33, 34]. So combined drugs that simultaneously affect multiple targets are more

beneficial to control complex disease, reverse drug resistance. For a compound, if it is a multi-target molecule and targets different proteins in different cell circumstance, the occurrence of resistance would also be decreased to minimum extent. We believed CPT is a multi-target compound as targeting the molecules such as STAT3[12], AMPK[15], MAPK[14], ER[16], NRF2[35] to prevent cancer growth has been proved. However, these proteins are not the final targets of CPT but the mediators because just ER and BCRP can be structurally bound with CPT. The Fig. 7 illustrates in detail the molecular process of CPT inhibition of BCRP by an ERα-dependent and -independent manner.

At present, designing the multi-target molecules based on the systems biology, structural biology and chemical informatics has become an optimum way to develop a new drug[34]. CPT as a multi-target compound would be a potential candidate drug plus with its selective BCRP inhibition in ERα$^-$ breast cancer. Meanwhile, the combination of CPT and anti-cancer drugs can enhance the sensitivity of cancer cells to chemotherapeutic drugs, and spread the range of their application in clinic. Additionally, although the inhibitory activity of CPT is not dominant compared to some current BCRP inhibitors, we expected CPT as a lead compound from natural herb, and after appropriate optimization of the structure in the later stage, will be develop to a highly effective and low-toxic natural BCRP-specific inhibitor to serve clinical therapy.

5. Conclusions

CPT is a novel natural BCRP inhibitor via blocking the formation of BCRP membrane dimer. At the presence of ERα, it functions via ERα regulation, but directly blocks BCRP at the absence of ERα in resistant cells. CPT can inhibit ERα-dependent and -independent BCRP, contributing to decrease the occurrence of resistance in breast cancer. It could be used in breast cancer with high expression of BCRP no matter whatever ERα expression.

Abbreviations

CPT Cryptotanshinone

BCRP Breast cancer resistance protein

ERα Estrogen receptor α

MDR Multidrug resistance

ABC ATP-binding cassette

MRP1 Multidrug-resistance-associated protein 1

NBD Nucleotide-binding domain

TMD Transmembrane domain

MX Mitoxantrone

DOX Doxorubicin

TOPO Topotecan

FRET Fluorescence resonance energy transfer

STAT3 Signal transducer and activator of transcription 3

AMPK Adenosine 5‘-monophosphate (AMP)-activated protein kinase

MAPK Mitogen-activated protein kinase

NRF2 Nuclear factor erythroid-2 related factor 2

Declarations

Ethics approval and consent to participate

Not applicable

Consent for publication

Not applicable

Availability of data and materials

All data generated or analysed during this study are included in this published article.

Competing interests

The authors declare that they have no conflict of interest.

Funding

The work was supported by Natural Science Foundation of Higher School of Jiangsu Province (17KJA360003, 18KJA360007), National Natural Science Foundation of China (No. 81673648, 81673725, 81673795, 81673852).

Authors' contributions

WC, YL provided the study design and supervision, and wrote the paper. WN, HF performed experiments and analyses. SW, SH assisted with molecular analysis and interpretation. XZ assisted with data analysis and statistic. FX, YW, XL and AW provided special reagents and/or helped in analyzing the experiments. All authors read and approved the final manuscript.

Acknowledgments

The work was supported by Natural Science Foundation of Higher School of Jiangsu Province (17KJA360003, 18KJA360007), National Natural Science Foundation of China (No. 81673648, 81673725, 81673795, 81673852).

References

1. Wang J, Seebacher N, Shi H, Kan Q, Duan Z. Novel strategies to prevent the development of multidrug resistance (MDR) in cancer. Oncotarget. 2017;8:84559–71.
2. Richman J, Dowsett M. Beyond 5 years: enduring risk of recurrence in oestrogen receptor-positive breast cancer. Nat Rev Clin Oncol. 2019;16:296–311.
3. Kathawala RJ, Gupta P, Ashby CR, Chen ZS. The modulation of ABC transporter-mediated multidrug resistance in cancer: a review of the past decade. Drug Resist Updat. 2015;18:1–17.
4. Mohammad IS, He W, Yin L. Understanding of human ATP binding cassette superfamily and novel multidrug resistance modulators to overcome MDR. Biomed Pharmacother. 2018;100:335–48.
5. Fletcher JI, Williams RT, Henderson MJ, Norris MD, Haber M. ABC transporters as mediators of drug resistance and contributors to cancer cell biology. Drug Resist Updat. 2016;26:1–9.
6. Lefèvre F, Boutry M. Towards Identification of the Substrates of ATP-Binding Cassette Transporters. Plant Physiol. 2018;178:18–39.
7. NMI T, Manolaridis I, Jackson SM, Kowal J, Stahlberg H, Locher KP. Structure of the human multidrug transporter ABCG2. Nature. 2017;546:504–9.
8. Johnson ZL, Chen J. Structural Basis of Substrate Recognition by the Multidrug Resistance Protein MRP1. Cell. 2017;168:1075–85.e9.
9. Mao Q, Unadkat JD. Role of the breast cancer resistance protein (BCRP/ABCG2) in drug transport–an update. AAPS J. 2015;17:65–82.
10. Horsey AJ, Cox MH, Sarwat S, Kerr ID. The multidrug transporter ABCG2: still more questions than answers. Biochem Soc Trans. 2016;44:824–30.
11. Li W, Zhang H, Assaraf YG, Zhao K, Xu X, Xie J, et al. Overcoming ABC transporter-mediated multidrug resistance: Molecular mechanisms and novel therapeutic drug strategies. Drug Resist Updat. 2016;27:14–29.
12. Shin DS, Kim HN, Shin KD, Yoon YJ, Kim SJ, Han DC, et al. Cryptotanshinone inhibits constitutive signal transducer and activator of transcription 3 function through blocking the dimerization in

DU145 prostate cancer cells. Cancer Res. 2009;69:193–202.

13. Chen W, Luo Y, Liu L, Zhou H, Xu B, Han X, et al. Cryptotanshinone inhibits cancer cell proliferation by suppressing Mammalian target of rapamycin-mediated cyclin D1 expression and Rb phosphorylation. Cancer Prev Res (Phila). 2010;3:1015–25.
14. Chen W, Liu L, Luo Y, Odaka Y, Awate S, Zhou H, et al. Cryptotanshinone activates p38/JNK and inhibits Erk1/2 leading to caspase-independent cell death in tumor cells. Cancer Prev Res (Phila). 2012;5:778–87.
15. Chen W, Pan Y, Wang S, Liu Y, Chen G, Zhou L, et al. Cryptotanshinone activates AMPK-TSC2 axis leading to inhibition of mTORC1 signaling in cancer cells. BMC Cancer. 2017;17:34.
16. Pan Y, Shi J, Ni W, Liu Y, Wang S, Wang X, et al. Cryptotanshinone inhibition of mammalian target of rapamycin pathway is dependent on oestrogen receptor alpha in breast cancer. *J Cell Mol Med* 2017.
17. Montanari F, Cseke A, Wlcek K, Ecker GF. Virtual Screening of DrugBank Reveals Two Drugs as New BCRP Inhibitors. SLAS Discov. 2017;22:86–93.
18. Xu J, Liu Y, Yang Y, Bates S, Zhang JT. Characterization of oligomeric human half-ABC transporter ATP-binding cassette G2. J Biol Chem. 2004;279:19781–9.
19. Ni Z, Mark ME, Cai X, Mao Q. Fluorescence resonance energy transfer (FRET) analysis demonstrates dimer/oligomer formation of the human breast cancer resistance protein (BCRP/ABCG2) in intact cells. Int J Biochem Mol Biol. 2010;1:1–11.
20. Zhang YK, Wang YJ, Lei ZN, Zhang GN, Zhang XY, Wang DS, et al. Regorafenib antagonizes BCRP-mediated multidrug resistance in colon cancer. Cancer Lett. 2019;442:104–12.
21. Mo W, Zhang JT. Oligomerization of human ATP-binding cassette transporters and its potential significance in human disease. Expert Opin Drug Metab Toxicol. 2009;5:1049–63.
22. Krapf MK, Gallus J, Vahdati S, Wiese M. New Inhibitors of Breast Cancer Resistance Protein (ABCG2) Containing a 2,4-Disubstituted Pyridopyrimidine Scaffold. J Med Chem. 2018;61:3389–408.
23. Herynk MH, Fuqua SA. Estrogen receptors in resistance to hormone therapy. Adv Exp Med Biol. 2007;608:130–43.
24. Berry DA, Cirrincione C, Henderson IC, Citron ML, Budman DR, Goldstein LJ, et al. Estrogen-receptor status and outcomes of modern chemotherapy for patients with node-positive breast cancer. JAMA. 2006;295:1658–67.
25. Koren E, Fuchs Y. The bad seed: Cancer stem cells in tumor development and resistance. Drug Resist Updat. 2016;28:1–12.
26. Chang FW, Fan HC, Liu JM, Fan TP, Jing J, Yang CL, et al. Estrogen Enhances the Expression of the Multidrug Transporter Gene ABCG2-Increasing Drug Resistance of Breast Cancer Cells through Estrogen Receptors. *Int J Mol Sci* 2017; 18.
27. Ee PL, Kamalakaran S, Tonetti D, He X, Ross DD, Beck WT. Identification of a novel estrogen response element in the breast cancer resistance protein (ABCG2) gene. Cancer Res. 2004;64:1247–51.

28. Yang M, Li H, Li Y, Ruan Y, Quan C. Identification of genes and pathways associated with MDR in MCF-7/MDR breast cancer cells by RNA-seq analysis. Mol Med Rep. 2018;17:6211–26.
29. Oh AS, Lorant LA, Holloway JN, Miller DL, Kern FG, El-Ashry D. Hyperactivation of MAPK induces loss of ERalpha expression in breast cancer cells. Mol Endocrinol. 2001;15:1344–59.
30. Campbell RA, Bhat-Nakshatri P, Patel NM, Constantinidou D, Ali S, Nakshatri H. Phosphatidylinositol 3-kinase/AKT-mediated activation of estrogen receptor alpha: a new model for anti-estrogen resistance. J Biol Chem. 2001;276:9817–24.
31. Peña-Solórzano D, Stark SA, König B, Sierra CA, Ochoa-Puentes C. ABCG2/BCRP: Specific and Nonspecific Modulators. Med Res Rev. 2017;37:987–1050.
32. Sonne-Hansen K, Norrie IC, Emdal KB, Benjaminsen RV, Frogne T, Christiansen IJ, et al. Breast cancer cells can switch between estrogen receptor alpha and ErbB signaling and combined treatment against both signaling pathways postpones development of resistance. Breast Cancer Res Treat. 2010;121:601–13.
33. Zimmermann GR, Lehár J, Keith CT. Multi-target therapeutics: when the whole is greater than the sum of the parts. Drug Discov Today. 2007;12:34–42.
34. Poornima P, Kumar JD, Zhao Q, Blunder M, Efferth T. Network pharmacology of cancer: From understanding of complex interactomes to the design of multi-target specific therapeutics from nature. Pharmacol Res. 2016;111:290–302.
35. Wang W, Wang X, Zhang XS, Liang CZ. Cryptotanshinone Attenuates Oxidative Stress and Inflammation through the Regulation of Nrf-2 and NF-κB in Mice with Unilateral Ureteral Obstruction. Basic Clin Pharmacol Toxicol. 2018;123:714–20.

Figures

A

Cell	Drug Concentration	CPT-5μmol/L (1.482μg/ml)	CPT-10μmol/L (2.964μg/ml)	CPT-20μmol/L (5.928μg/ml)
MCF-7	Intracellular	1.265±0.033	2.779±0.056	5.897±0.097
	Extracellualr	1.286±0.005	2.570±0.034	5.624±0.104
MDA-MB-231	Intracellular	1.038±0.010	1.871±0.056	1.304±0.065
	Extracellualr	1.436±0.147	2.686±0.532	5.556±0.072

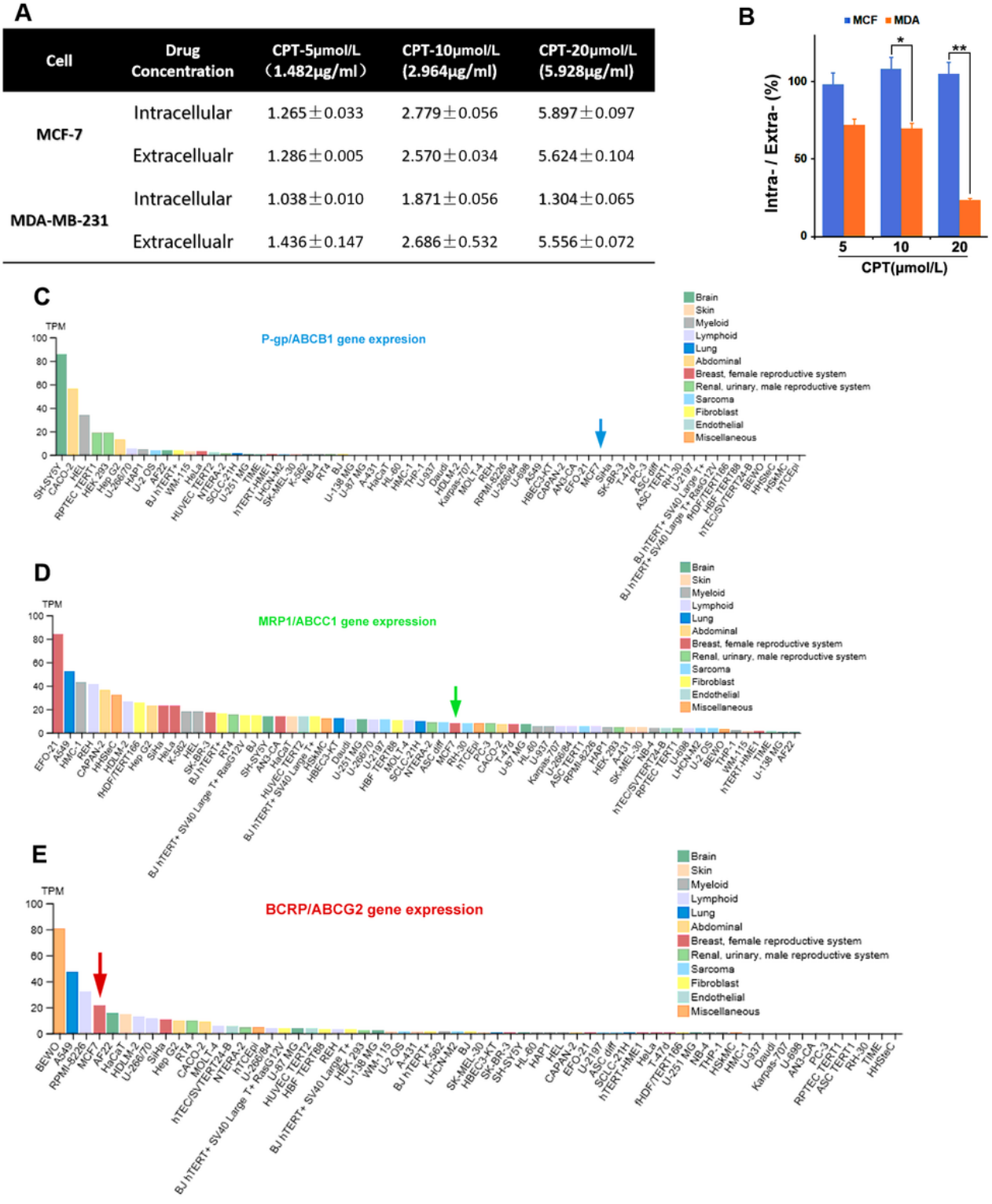

Figure 1

That CPT accumulates intracellular side in MCF-7 cells is possibly related to BCRP (A) The breast cancer cells were treated with CPT (5, 10, 20 μmol/L) for 8 hrs, then collected the medium and cellular lysates respectively for HPLC analysis of the intracellular and extracellular CPT concentration. The data are presented as Mean ±SD (n=3). (B) statistical analysis of the ratio of intracellular CPT/Extracellular

CPT×100%, n=3, *P<0.05, **P<0.01. (C, D, E) The expression of gene ABCB1/ABCC1/ABCG2 mRNA levels in different cells based on the Human Protein Atlas database analysis.

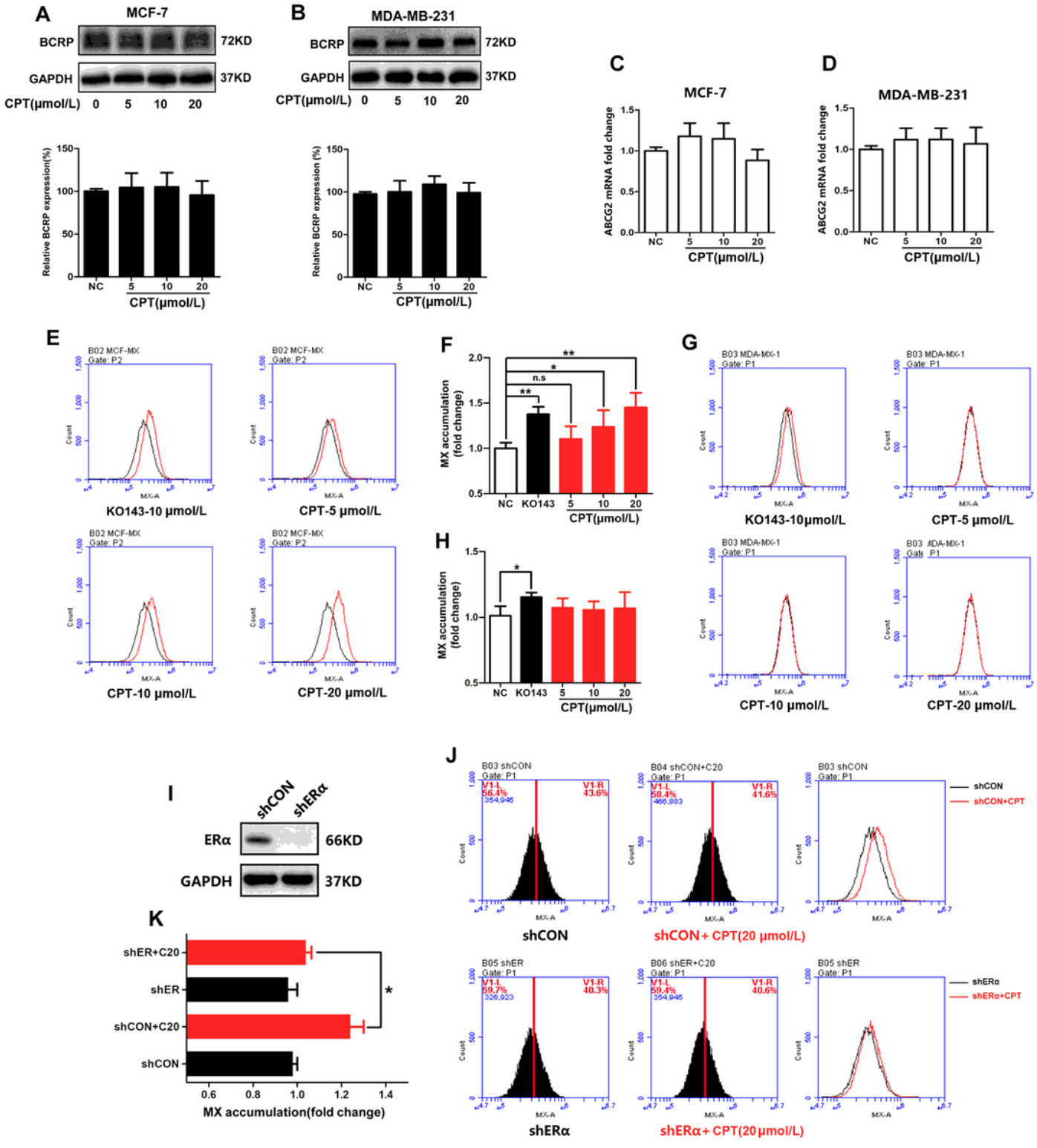

Figure 2

CPT inhibits efflux function of BCRP in MCF-7 cells Western blot analysis of the protein expression of BCRP in MCF-7 cells (A) and MDA-MB-231 cells (B) treated with CPT for 8h. Q-PCR analysis of the transcription expression of BCRP in MCF-7 cells (C) and MDA-MB-231 cells (D) treated with CPT for 8h.

The MX fluorescence accumulation was detected in MCF-7 cells (E) and MDA-MB-231 cells (G) treated with CPT for 8h by the flow cytometry FL-4 channel, and the fluorescence intensity represents the activity of BCRP efflux. The quantitated results were indicated in (F) and (H) respectively, versus negative control (NC), n=3, *P<0.05, **P<0.01. (I) MCF-7 cells with shCON or with shERα were respectively treated with or without CPT (20 μmol/L) for 8h and then (J) analyzed MX fluorescence accumulation via flow cytometry FL-4 channel. The quantitated results were indicated in (K), n=3, *P<0.05.

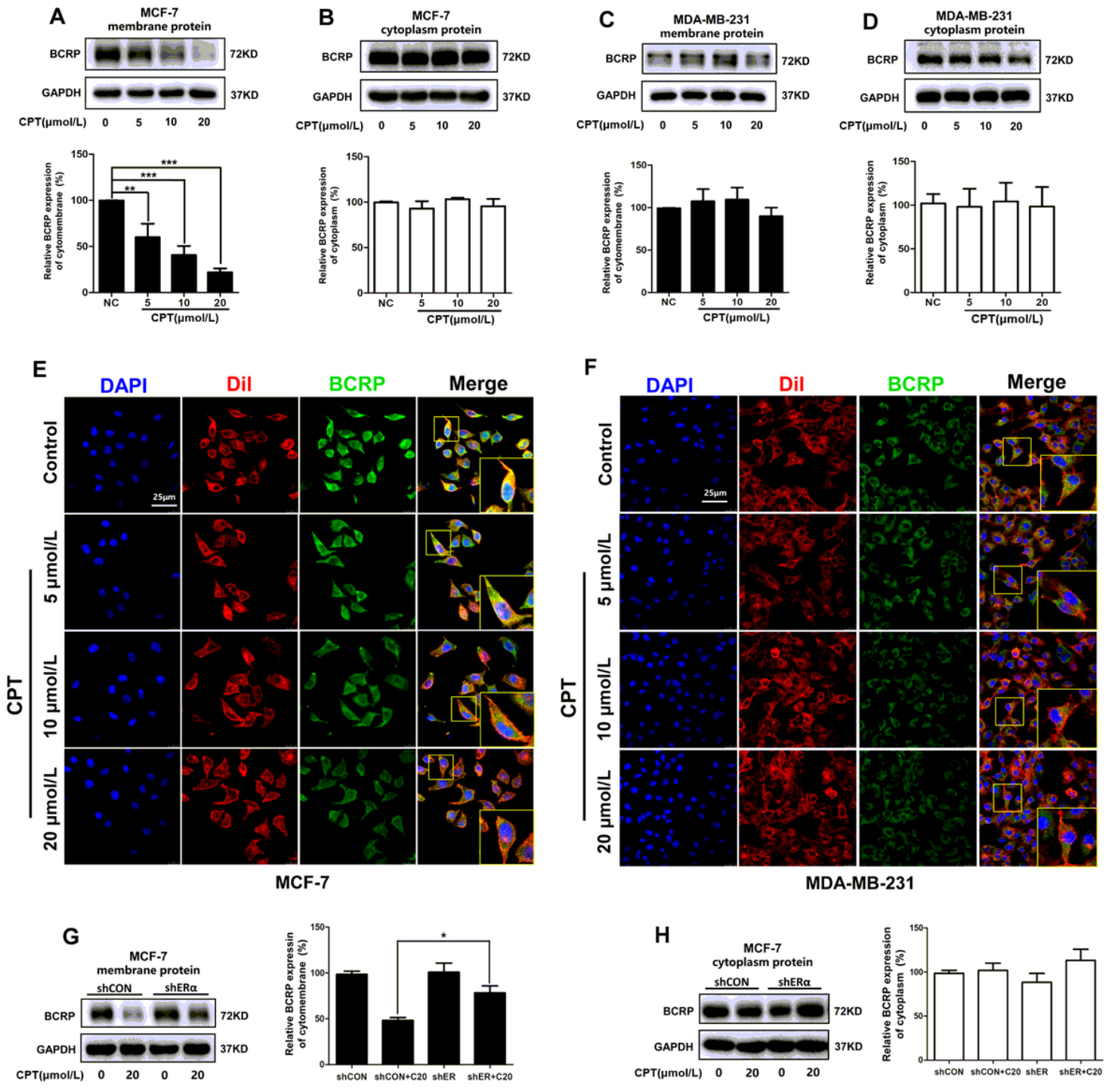

Figure 3

CPT can reduce membrane expression and localization of BCRP in MCF-7 cells Western blot analysis of the BCRP cell membrane and cytoplasm protein expression in MCF-7 cells (A, B) and MDA-MB-231 cells (C, D) treated with CPT for 8h. versus negative control (NC), n=3, **P<0.01, ***P<0.001. Immunofluorescence staining for BCRP in MCF-7 (E) and MDA-MB-231 (F) cells which treated with CPT for 8h, and cell membrane labeled with DiI. Scale bar, 25μm. (G, H) MCF-7 cells with shCON or with shERα were respectively treated with or without CPT (20μmol/L) for 8h and then cell membrane protein or cytoplasm protein were extracted to analyze the expression of BCRP.

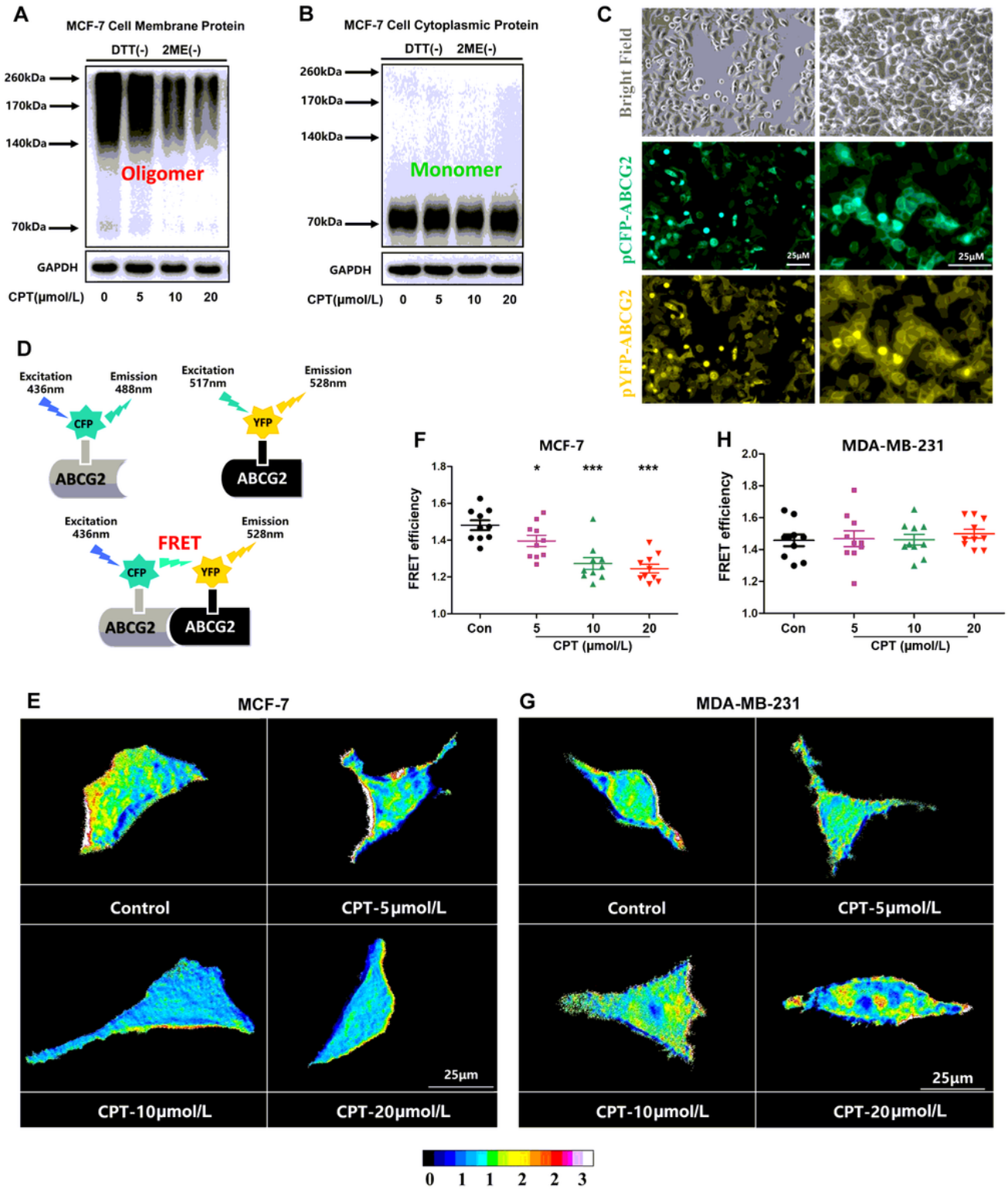

Figure 4

CPT inhibits BCRP oligomer formation in MCF-7 cells (A, B) CPT was given as described previously, the membrane proteins or cytoplasm protein were extracted to detect the oligomer of BCRP under non-reducing condition. (C) After transfection of pCFP-ABCG2 and pYFP-ABCG2 in MCF-7 cells for 24h, the expression of BCRP on the cell membrane was observed under 200X and 400X magnification. (D) Schematic diagram of FRET experiment, pCFP and pYFP are the donor and acceptor of fluorescence energy respectively. When their distance reached within 10nm, the FRET phenomenon would happen. FRET was applied to analyze the oligomer of BCRP in MCF-7 cells (E, G) and MDA-MB-231 cells (F, H) treated with CPT in the state of living cells. Images were exhibited as 16 colors map, and the color represents the degree of FRET efficiency. The quantitated data of FRET are versus control, n=10, *P<0.05, ***P<0.001.

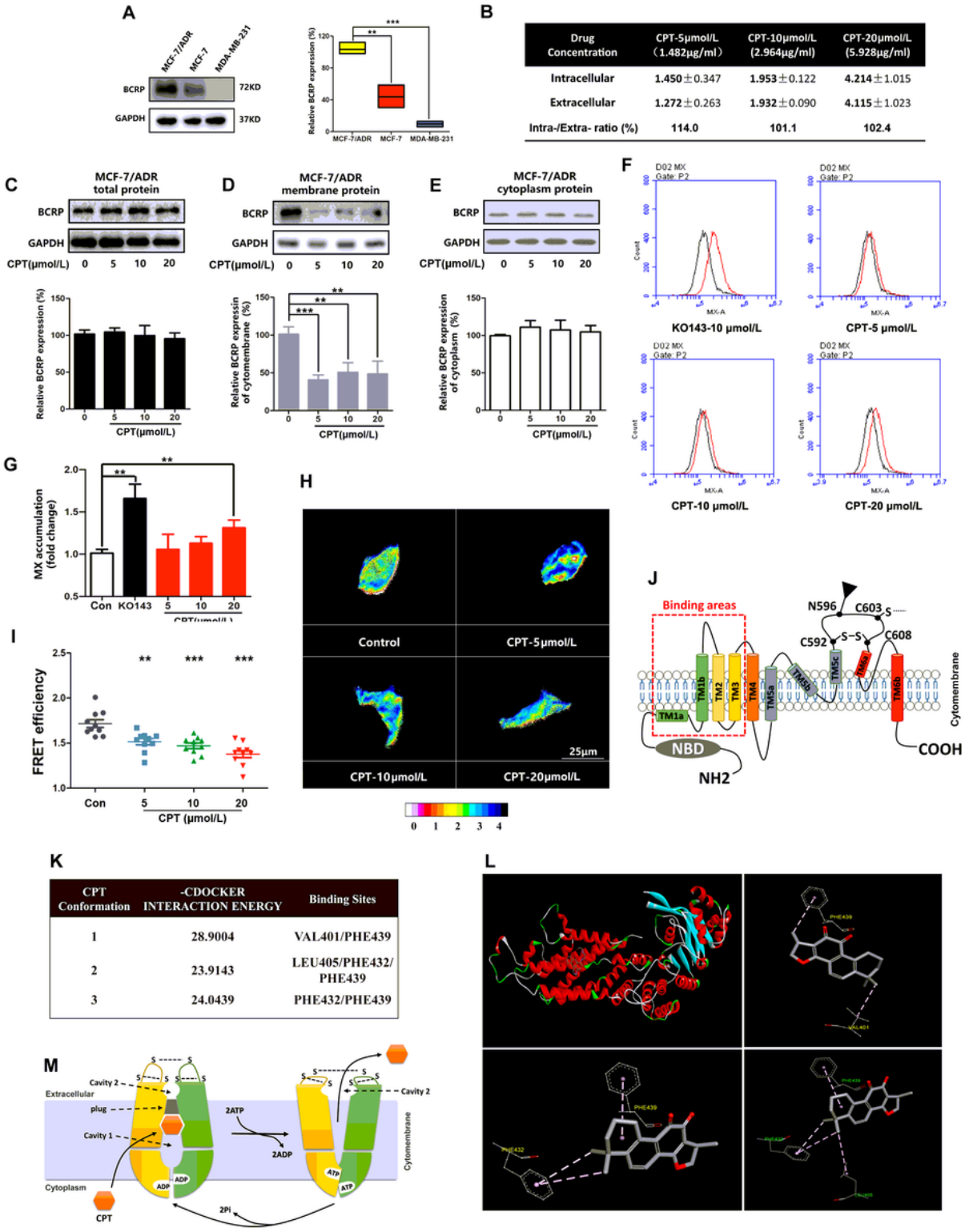

Figure 5

CPT inhibits membrane expression and function of BCRP in MCF-7/ADR cells (A) Western blot analysis of the BCRP in different breast cancer cells. N=3, **P<0.01. (B) HPLC analysis of the concentration of intracellular and extracellular CPT in MCF-7/ADR cells which treated with CPT for 8h. The data are presented as Mean ± SD. Western blot analysis of the BCRP total protein (C), membrane protein (D), cytoplasm protein (E) expression of in MCF-7/ADR cells treated with CPT for 8h. (F) MX fluorescence

accumulation was detected by the flow cytometry FL-4 channel in MCF-7/ADR cells which treated with CPT for 8h, and (G) The quantitated data were versus control, n=3, **P<0.01. (H) FRET analysis of the oligomer of BCRP in MCF-7/ADR cells which treated with CPT in the state of living cells. Images were exhibited as 16 colors map, and the color represents the degree of FRET efficiency. (I) The quantitated data were versus control, n=10, **P<0.01, ***P<0.001. (J) Schematic diagram of BCRP protein structure, TM1, TM2, TM3 are substrate binding regions. (K) The molecular docking analysis about the sites of CPT docking with BCRP and their interaction energy. (L) The 3D structure of CPT docking with BCRP substrate binding pocket, and three stable conformations and binding sites are listed. (M) The whole process of BCRP transporting substrates.

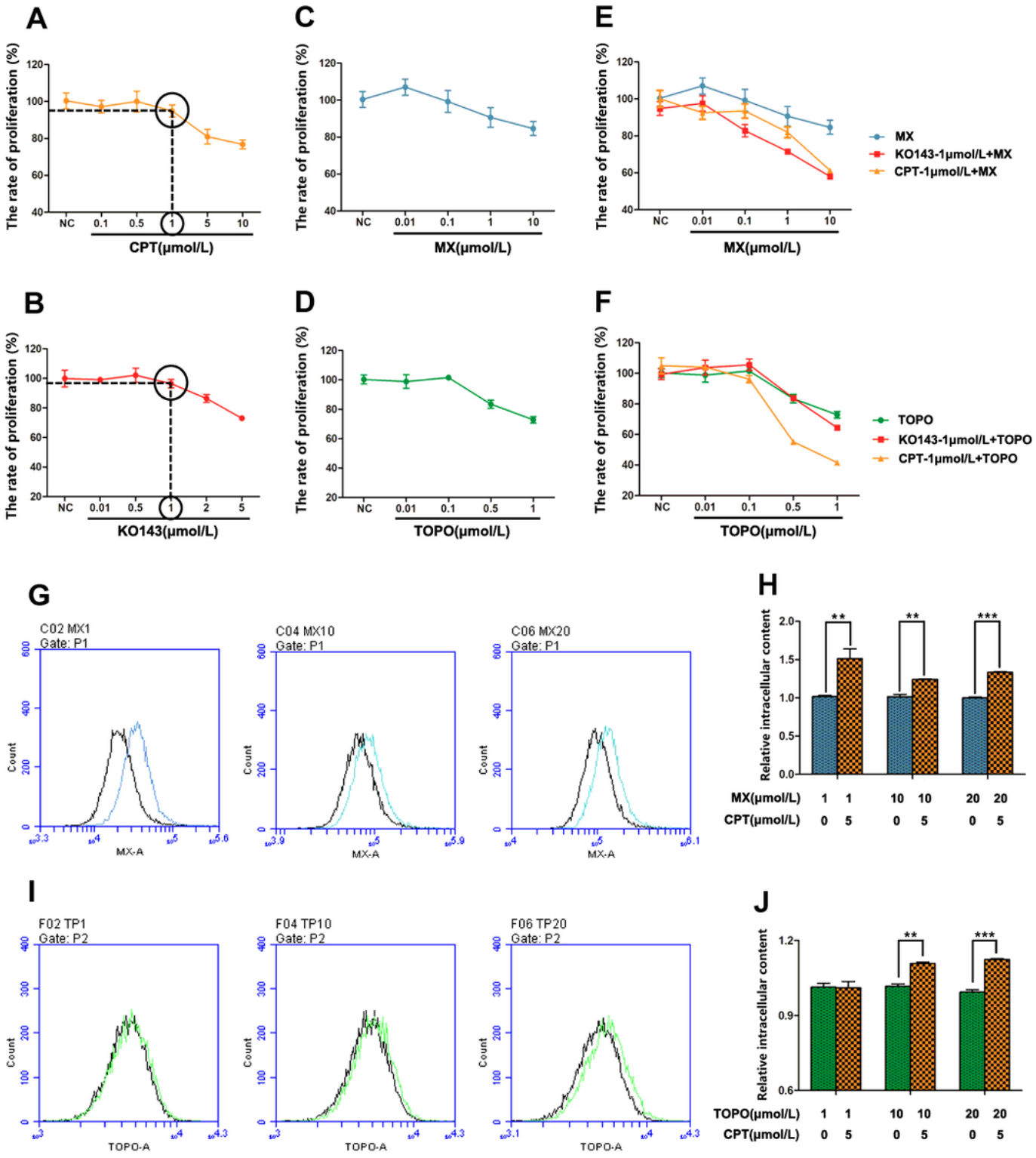

Figure 6

CPT combined with BCRP efflux anti-cancer drugs can enhance cancer cell sensitivity MCF-7/ADR cells were respectively treated with CPT (A) or KO143 (B) for 72h to screen the highest concentration that does not significantly affect cell proliferation. MCF-7/ADR cells were treated with mitoxantrone (C) and topotecan (D) for 72h to test cell viability. (E) Cell proliferation of MCF-7/ADR cells treated with mitoxantrone and KO143-1μmol/L+mitoxantrone and CPT-1μmol/L+mitoxantrone for 72h. (F) Cell

proliferation of MCF-7/ADR cells treated with topotecan and KO143-1μmol/L+topotecan and CPT-1μmol/L+topotecan for 72h. Mitoxantrone (MX) (G) and topotecan (TOPO) (H) fluorescence accumulation were detected by the flow cytometry FL-4 channel in MCF-7/ADR cells respectively treated with CPT+MX or CPT+TOPO for 8h, and the fluorescence intensity reflects the relative content of intracellular drugs. (I) Comparison of intracellular MX content in CPT+MX group and MX alone group in MCF-7/ADR cells for 8h. Results were versus MX alone respectively, n=3, **P<0.01, ***P<0.001. (J) Comparison of intracellular TOPO content in CPT+TOPO group and TOPO alone group in MCF-7/ADR cells for 8h. Results were versus TOPO alone respectively, n=3, **P<0.01, ***P<0.001.

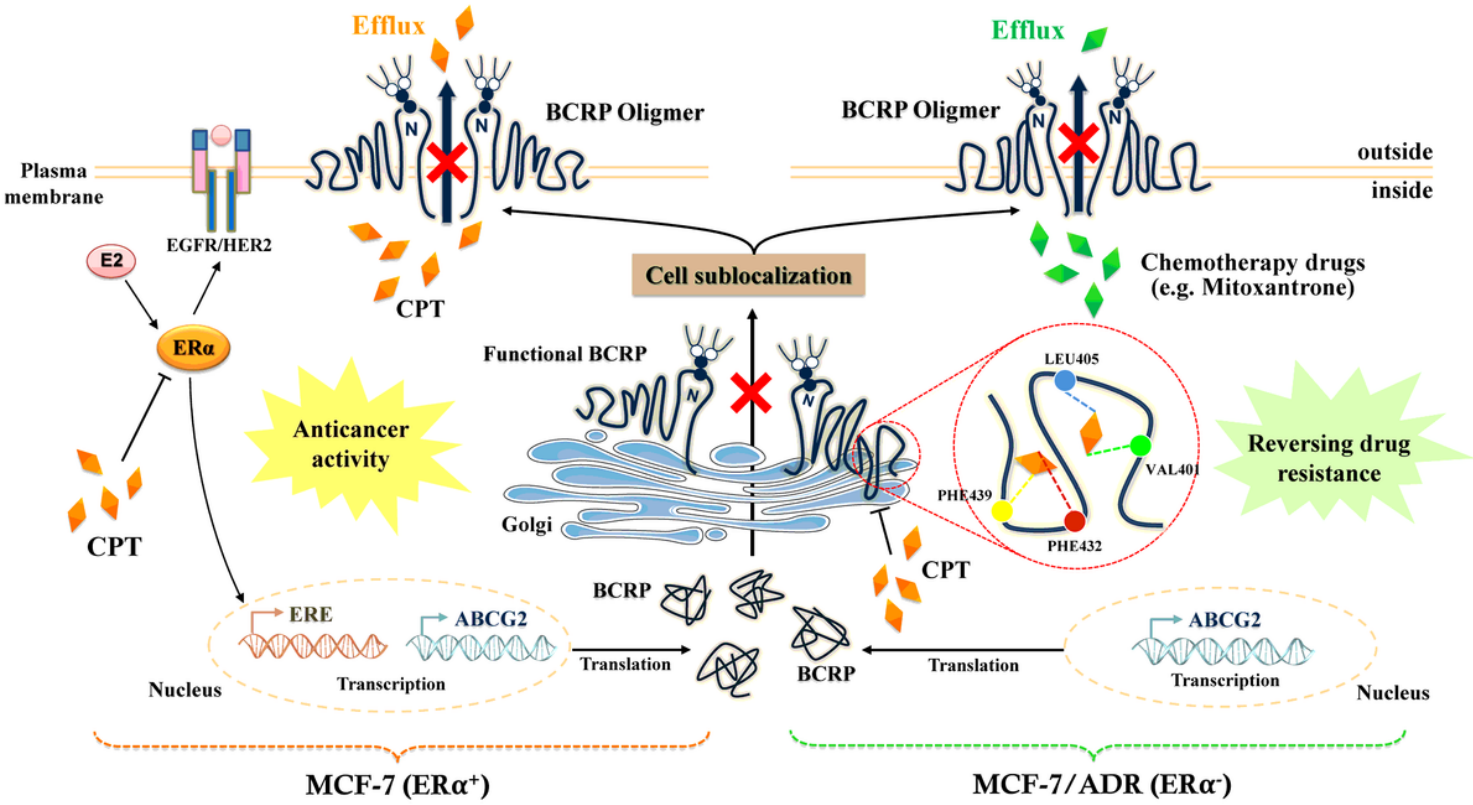

Figure 7

Effect of CPT on P-gp and MRP1 protein expression and efflux function in MCF-7/ADR cells Western blot analysis of the P-gp and MRP1 cell membrane protein expression (A) and cytoplasm protein expression (C) in MCF-7/ADR cells treated with CPT for 8h, and the corresponding semi-quantitation analysis was indicated in (B) and (D). RH123 (E) and DOX (F) fluorescence accumulation in MCF-7/ADR cells treated with CPT for 8h were respectively detected by the flow cytometry FL-1 channel, and the fluorescence intensity represents the activity of P-gp and DOX efflux. RH123 and DOX were respectively the substrate of P-gp and MRP1. (G) The quantitated data of (E) and (F).

Supplementary Files

This is a list of supplementary files associated with this preprint. Click to download.

- FIGURES21.tif
- FIGURES21.tif
- FIGURES11.tif
- FIGURES11.tif
- TableS1.docx
- TableS1.docx